Sociobiology
An international journal on social insects

RESEARCH ARTICLE - TERMITES

Transcriptional Response of the Termite *Coptotermes formosanus* to Infection by the Entomopathogenic Fungus *Akanthomyces lecanii*

Kai Feng[1], Qi Ye[1], Yiyang Zhao[1], Liang Liu[1], Yueqiu He[1], Wen Li[1], Feilong Yu[1], Zhilong Wang[1], Weigang Chai[2]

1 - Ningbo Key Laboratory of Ornamental Plant Genetics, Breeding and Utilization, College of Landscape and Ecology, NingBo City College of Vocational Technology, Ningbo 315000, China

2 - Ningbo Academy of Agricultural Sciences, Ningbo 315000, China

Article History

Edited by
Og De Souza, UFV, Brazil
David Sillan-Dussès, Univ. Paris 13, France
Received 28 October 2025
Initial acceptance 18 February 2026
Final acceptance 06 May 2026
Publication date 20 July 2026

Keywords
Termite, immune response, metabolism, fungal infection.

Corresponding author
Kai Feng
College of Landscape and Ecology, NingBo City College of Vocational Technology, 7 Fengling Road, Ningbo 315000, China.
E-Mail: 1012609289@qq.com

Abstract

Coptotermes formosanus, a worldwide pest, inflicts large losses on agriculture, forestry, construction, and other industries. As efficient, environmentally friendly pest control methods, microbial biopesticides are widely used to manage major pests. We previously isolated an *Akanthomyces lecanii* strain with strong insecticidal activity against termites. However, the interaction between the biocontrol agent and termites is still unknown. In this study, PacBio single-molecule real-time (SMRT) sequencing technology and Illumina RNA-seq sequencing technology were used to explore the transcriptomic differences in *C. formosanus* before and after *A. lecanii* infection. A total of 7,882,407 full-length transcripts were obtained. Single genes were further annotated using the NR, GO, KEGG, COG/KOG, Swiss-Prot, and KEGG homology public databases. A total of 2,782 differentially expressed genes were identified, including 1,440 upregulated genes and 1,342 downregulated genes. The expression of the Toll signaling pathway, mitogen-activated protein kinase (MAPK) pathway, detoxification metabolism, and immune-related genes, including scavenger receptor, apolipophorin, Cdc42, Integrin, Toll, serine protease, and transferrin genes, may be related to *A. lecanii* infection. This work not only greatly enriches the gene annotation resources of *C. formosanus* but also provides a new perspective for understanding the fungal immune defense mechanisms of social insects at the molecular level. These findings provide a theoretical basis for the development of new immunosuppressive agents.

Introduction

Termites, such as bees and ants, are social insects. Current research has shown that termites play important roles in the global carbon cycle, especially in tropical and subtropical ecosystems (Xue et al., 2024). However, they remain a devastating pest worldwide. *Coptotermes formosanus* (Shiraki) is among the most widely distributed termites in tropical and subtropical regions and has strong plasticity and diffusion force (Kalleshwaraswamy et al., 2022; Sharma et al., 2025). *C. formosanus* can damage all types of wood materials and living trees, thus disrupting and harming the human economy and ecology.

Currently, to minimize termite-related losses to humans, significant manpower, material resources, and financial investments have been devoted to termite control. Imidacloprid, fipronil, chlorpyrifos, fenvalerate, and bifenthrin are commonly used as termite control pesticides. Although chemical control can achieve certain results, it can leave pesticide residues, posing serious harm to the ecological environment. Moreover, with growing awareness of environmental protection, green pesticides are becoming increasingly favored. Insect pathogenic fungi are important biological control agents that have always been a research hotspot due to their green and environmentally friendly nature. *Akanthomyces lecanii* (Zimm.) Spatafora, Kepler & B. Shrestha (*Verticillium lecanii* (Zimm.) Viégas), is an

important biocontrol fungus that has an extensive host range (Kepler et al., 2017). Notably, this fungus has been developed as an important biological control agent and is widely used to control major agricultural pests such as aphids, whiteflies, and scale insects (Sharma et al., 2023). In our previous study, we isolated a fungus with high termite killing activity from *C. formosanus*, which died naturally and had white hairs on its body surface. Through morphological and molecular biological identification, the isolate was confirmed as *A. lecanii*, which we named NBCC-L5. Although *A. lecanii* has been reported as a broad-spectrum entomopathogenic fungus, no studies have reported how it interacts with termites, especially at the molecular and transcriptional levels.

In recent years, to obtain more accurate data for functional genome research on insect species, third-generation high-throughput sequencing technology characterized by single-molecule real-time (SMRT) sequencing has been used, including for *Erthesina fullo* (Thunberg) (Jia et al., 2018), *Agasicles hygrophila* Selman and Vogt (Gao et al., 2016), *Odontotermes formosanus* (Shiraki) (Feng et al., 2020), and *Coridius chinensis* (Dallas) (Xu et al., 2023). Compared with second-generation sequencing platforms, third-generation technologies offer distinct advantages, such as longer read lengths and the ability to capture full-length transcripts without assembly, thereby greatly improving the accuracy of gene structure and functional annotation. In a study of termite immunogenomics, Chen et al. (2023) systematically identified immune-related genes in *C. formosanus* infected with *M. anisopliae* through whole-genome analysis. However, the immune response mechanism of *C. formosanus* during *A. lecanii* infection has not yet been reported using full-length sequencing. In this study, the full-length transcriptomes of infected (*A. lecanii*) and uninfected *C. formosanus* were sequenced to identify key pathways and genes involved in the immune response. This study provides a theoretical basis for understanding the molecular mechanism underlying *C. formosanus* resistance to *A. lecanii* infection and for termite control strategies based on *A. lecanii*. Furthermore, this study provides a theoretical basis for the development of new immunosuppressive agents.

Materials and methods

Insects and pathogenic bacteria

3 colonies of *C. formosanus* were collected from Ningbo, Zhejiang Province, China. The harvested nests were maintained in an insect growth chamber under constant darkness (L:D = 0:24) at 27 ± 1 °C and 50 ± 1% relative humidity. The *A. lecanii* strain NBCC-L5, originally isolated from naturally infected and deceased *C. formosanus* workers, was preserved at 4 °C until use.

Sample processing

Potato dextrose agar medium was used as the inoculation medium, and *A. lecanii* strain NBCC-L5 was inoculated onto the medium for culture at 27 °C for 3 days. A punch was used to pick up the *A. lecanii* block from the edge of the colony on solid medium, which was subsequently transferred to PDA liquid medium and cultured on a shaker at 27 °C for 2 days to obtain spores. The resulting fungal suspension was filtered to obtain conidia, which were subsequently diluted with sterile distilled water to a final concentration of 1.5×10^9 conidia·mL^{-1} for subsequent experiments.

Termite infection assays were conducted using the droplet application method. The sterilized filter paper was laid on the bottom of a 6 cm sterile Petri dish, and an appropriate amount of sterile water was added to keep it wet. Twenty healthy and mature worker termites of *C. formosanus* were placed in each dish. For the infection treatment group (TT), 0.1 μL of *A. lecanii* conidia was pipetted using a micropipette to drop the suspension on the pronotum of each termite. For the control group (CK), 0.1 μL of sterile water was added dropwise using the same method. Termites were treated for 12 h, after which samples were collected in groups. The collected termite samples were immediately flash frozen in liquid nitrogen for subsequent analysis. Termites were collected from three independent colonies. For each treatment, three biological replicates were established (e.g., A + B + C). In each replicate, individuals from the three colonies were combined (e.g., A1 + B1 + C1) to generate one pooled sample. This pooling strategy was used to reduce colony-specific variation. A total of three pooled samples were obtained for each treatment.

RNA sample preparation

Total RNA was extracted from termite tissue samples using a standardized protocol for third-generation sequencing. To obtain accurate data, the RNA concentration and purity were measured using a NanoDrop 2000 spectrophotometer (Thermo Fisher Scientific, USA). Moreover, RNA integrity was detected by agarose gel electrophoresis, and genomic DNA contamination was detected. In addition, RNA integrity was numerically evaluated using an Agilent 2100 Bioanalyzer (Agilent Technologies, USA). The combined application of the above detection methods provides reliable data support for subsequent experiments. The basic prerequisite for obtaining effective transcriptome data is the utilization of high-quality RNA materials. First, the RNA purity (OD260/280), concentration, and shape of the nucleic acid absorption peaks were evaluated using NanoDrop measurements. Each library requires at least 1 μg of total RNA with a concentration ≥ 200 ng·μL^{-1} and an OD260/280 ratio between 1.8 and 2.2. Afterward, an Agilent 2100 Bioanalyzer was used to evaluate RNA integrity on the basis of the Rin value, 28S/18S rRNA ratio, baseline spectrum, and 5S rRNA peak. Finally, agarose gel electrophoresis was used to visually confirm RNA integrity and ensure no contamination. Only samples that meet the above criteria and pass the test can be used for subsequent sequencing and data analysis.

Library preparation and SMRT sequencing

Quality control was performed using RNA exemplars, and comprehensive cDNA repositories were constructed, with the Iso-Seq Express 2.0 procedural methodology (PacBio, USA) adhered to during execution. Using barcode primers, the mRNA strand was processed into full-length cDNA by reverse transcription and a subsequent amplification process, and the cDNA barcode was incorporated at the 5' end. The amplified cDNA products were then purified using SMRTbell® cleanup beads. The purified cDNA was quantified with a Qubit 3.0 fluorometer (Thermo Fisher Scientific, USA). Afterward, the fragment size distribution was analyzed and detected using an Agilent 2100 Bioanalyzer (Agilent Technologies, USA).

The Kinnex™ PCR 8-fold Kit (PacBio, USA) was subsequently used for Kinnex PCR amplification and pooling, followed by purification of the combined PCR products. Using the scheme provided by the manufacturer, the Kinnex™ Concatenation Kit was selected for further processing of cDNA to obtain long fragments. These fragments were end-repaired, adaptor-ligated, nuclease-treated, and purified with SMRTbell® cleanup beads to produce the final SMRTbell® libraries for sequencing.

A Qubit 3.0 fluorometer was used to quantitatively analyze the library, and an Agilent Femto Pulse system (Agilent Technologies, USA) was used to analyze and detect the fragment size distribution. Only libraries with concentrations and fragment size profiles meeting the quality requirements were subjected to PacBio sequencing.

Sequel data output and quality control

Raw sequencing data were preprocessed using the SMRT Link software suite (PacBio, USA), and full-length transcript sequences were obtained through the Iso-Seq analysis workflow. In brief, subreads were generated by polymerase read demultiplexing, and subreads derived from the same polymerase read were self-corrected to produce high-quality circular consensus sequences (CCSs). A CCS is defined as a low-error-rate sequence generated from at least two sequencing passes within a single zero-mode waveguide (ZMW), with base accuracy exceeding a predetermined threshold.

CCS reads were subsequently screened for concatemers and the presence of 5' and 3' primers to classify them into distinct categories, including full-length (FL), full-length nonconcatemer (FLNC), and polyadenylated FLNC sequences. Only FLNC reads containing both the 5' primer, 3' primer, and a poly(A) tail in the correct order were retained for downstream analysis. Two FLNC reads were clustered together if they satisfied all three criteria simultaneously: a 5'-end length difference of less than 100 bp, a 3'-end length difference of less than 30 bp, and internal gap lengths shorter than 10 bp.

Eukaryotic genes often undergo alternative splicing; therefore, multiple FLNC reads can represent different isoforms of the same gene. Nonredundant transcript sets were obtained by clustering and collapsing FLNC reads using the iterative clustering and error correction (ICE) module implemented in SMRT Link. The arrow algorithm was subsequently used to analyze and process the obtained consensus transcripts, thereby improving sequence accuracy. When short-read transcriptome data were available, additional error correction was performed using the LoRDEC program, leveraging second-generation data to refine the polished transcripts. Finally, redundant sequences were removed using cd-hit clustering, and the resulting high-confidence, full-length transcript set was used for subsequent analyses and as the reference for short-read alignment.

Functional annotation of transcripts

NR, GO, KEGG, COG/KOG, and Swiss-Prot are the five most commonly used databases. All full-length transcripts were compared with them to obtain functional annotations. To identify homologous proteins with the highest sequence similarity, the DIAMOND BLASTx tool was used to search these databases. The Non-Redundant Protein Sequence (NR) and Swiss-Prot databases are two of the most widely used protein resources, with Swiss-Prot providing manually curated and nonredundant protein entries to ensure high annotation accuracy. The COG/KOG database (Clusters of Orthologous Groups for prokaryotes and eukaryotes, respectively) classifies gene products on the basis of orthology, with each COG or KOG protein cluster representing an inferred ancestral protein shared among organisms with complete genomes, such as bacteria, algae, and eukaryotes.

First, the genes in the data were aligned with Gene Ontology (GO) to clarify gene function. To clarify gene function, we first performed Gene Ontology (GO) annotation on the gene products. This annotation system defines gene attributes according to three core levels: biological process (BP), molecular function (MF), and cellular component (CC) categories. Finally, owing to the system of unique identifiers, GO annotations support functional comparison and classification within hierarchical databases.

Kyoto Encyclopedia of Genes and Genomes (KEGG) annotation, which enables mapping of counts of quantitative transcripts to known metabolic and signaling pathways, enables systematic analysis of biological roles and interactions of gene products in cellular processes. Together, the annotations provide integrated levels of understanding of the molecular means and biological significance of full-length transcripts in *C. formosanus*.

Digital gene expression library preparation and analysis

Transcript quantification was performed using RSEM software, and Bowtie2 software was used in the sequence alignment phase. The number of reads mapped to each transcript was calculated within each sample, and the isomer expression levels were normalized using fragments per kilobase of transcript per million mapped reads (FPKM) values. Notably, this method treats paired end reads from the same segment as a single

segment for processing. The influence of sequencing depth and transcription length has been accounted for by the FPKM index, and examples show that it has high accuracy in estimating the abundance of homologous expression.

Differential gene expression was obtained by analyzing transcript data using the DESeq2 software package. To compare transcriptional changes between the *A. lecanii*-infected group (TT) and the control group (CK), we applied a statistical test corrected for multiple comparisons using the false discovery rate (FDR) method. Genes were regarded as significantly differentially expressed when the FDR value was less than 0.05 and the absolute value of the $\log_2$ fold change ($|\log_2 FC|$) exceeded 1. Following the identification of DEGs, functional enrichment analyses were carried out. Gene Ontology (GO) annotations were used to classify genes into biological process, molecular function, and cellular component categories. In parallel, Kyoto Encyclopedia of Genes and Genomes (KEGG) pathway analysis was employed to identify the signaling and metabolic pathways involved in termites' immune response to fungal infection.

Results

SMRT sequencing data output

A total of 7,898,136 circular consensus sequences (CCSs) were obtained from the data after PacBio SMRT sequencing technology was used (Table 1). A CCS represents a high-quality sequence obtained from at least two passes of the same zero-mode waveguide (ZMW) read, with sequencing errors corrected through multiple rounds of self-consensus. Owing to the differences in the presence and location of the 5' primer, 3' primer, and poly(a) tail, the CCS reads were divided into three categories in total, with the number of each category also differing: 7,897,914 full-length (FL) reads, 7,886,313 full-length nonconcatemer (FLNC) reads, and 7,882,407 polyadenylated FLNC reads. In total, 7,882,407 FLNC reads, with an average length of 1,876 bp and an N50 of 1,913 bp, were obtained and used for downstream analyses (Table 2). Eukaryotic genes often undergo alternative splicing; therefore, a single gene may produce multiple transcript isoforms, and repeated sequencing of the same transcript can yield multiple FLNC reads. All FLNC reads were clustered and collapsed by the iterative clustering and error correction (ICE) tool in SMRT Link software, thereby rapidly yielding a nonredundant transcript set. The resulting consensus transcripts were further polished using the arrow algorithm, yielding 1,708,016 polished transcripts with an average length of 2,056 bp and an N50 length of 2,259 bp.

Transcript clustering analysis

Transcripts were further clustered, and redundant data were removed using the CD-HIT program, resulting in a final set of 783,142 nonredundant isoforms with an average length of 2,048 bp and an N50 length of 2,285 bp. These high-quality full-length isoforms were used for subsequent analyses and served as reference transcript sequences for short-read alignment.

Functional annotation of transcripts

A total of 783,142 transcripts were successfully annotated into different databases. Among them, 381,736 transcripts were successfully matched to the Gene Ontology (GO) database, 304,191 transcripts were matched to the KEGG (KO) database, 267,929 transcripts were matched to the KOG database, 306,092 transcripts were annotated in the Swiss-Prot database, and 515,828 transcripts were matched to the NR database. Moreover, 263,207 transcripts remained unannotated across the five databases, suggesting the presence of potentially novel or species-specific genes in *C. formosanus*.

In the NR database, the majority of the annotated transcripts were homologous to *C. formosanus* (283,868; 55.03%), followed by *Cryptotermes secundus* (Hill) (98,309; 19.06%), *Zootermopsis nevadensis* (Hagen) (32,463; 6.29%), *Blattella germanica* (L.) (12,107; 2.35%), *Spodoptera litura* (Fabricius) (3,251; 0.63%), *Cyprideis torosa* (Jones) (2,711; 0.53%), *Ephemera danica* Müller (2,430; 0.47%), *Stylophora pistillata* (Esper) (2,165; 0.42%), *Araneus ventricosus* (L. Koch) (2,075; 0.40%), and *Nymphon striatum* Losina-Losinsky (1,766; 0.34%) (Fig 1).

The data were analyzed using Blast2GO software through Gene Ontology (GO), and the *C. formosanus* transcriptomes were annotated into three main functional categories for classification. A total of 381,736 unigenes were assigned to 45 GO terms (Fig 2). In the biological process (BP) category,

Table 1. Statistics of CCS. Total bases (bp), the number of bases in the data; Total Number, the number of CCS; Minimum length, the minimum length of CCS; Average length, the average length of CCS; Maximum length, the maximum length of CCS; N50, the length of N50 after filtration.

Sample	Total_bases (bp)	Total number	Minimum length	Average length	Maximum length	N50
C. formosanus	14,810,098,723	7,898,136	155	1,876	19,597	1,913

Table 2. Statistics of FLNC. Total bases(bp): the number of bases in FLNC; Total Number: the total number of FLNC; Minimum length: the minimum length of FLNC; Average length: the average length of FLNC; Maximum length: the maximum length of FLNC; N50 (bp): the N50 length.

Sample	Total bases (bp)	Total number	Minimum length	Average length	Maximum length	N50
C. formosanus	13,933,275,012	7,882,407	50	1,768	8,870	1,825

the most abundant subcategories were cellular process (158,402), metabolic process (113,919), and biological regulation (47,235). In the cellular component (CC) category, the dominant subcategories were cellular anatomical entity (25,813), metabolic process (113,919), and protein-containing complex (39,798). Within the molecular function (MF) category, binding (189,401), catalytic activity (172,088), and transporter activity (33,983) were the most represented terms.

Furthermore, 267,929 sequences were successfully annotated in the KOG database and classified into 26 functional groups. The top three groups are general function prediction only (52,200), signal transduction mechanisms (35,119), and posttranslational modification, protein turnover, and chaperones (25,940) from top to bottom (Fig 3). The relatively limited representation of *C. formosanus* in the KOG database may reflect the scarcity of termite genomic data currently available. In addition, the identification of 263,207 unannotated transcripts suggests the existence of a considerable number of *C. formosanus*-specific genes whose functions are not yet known.

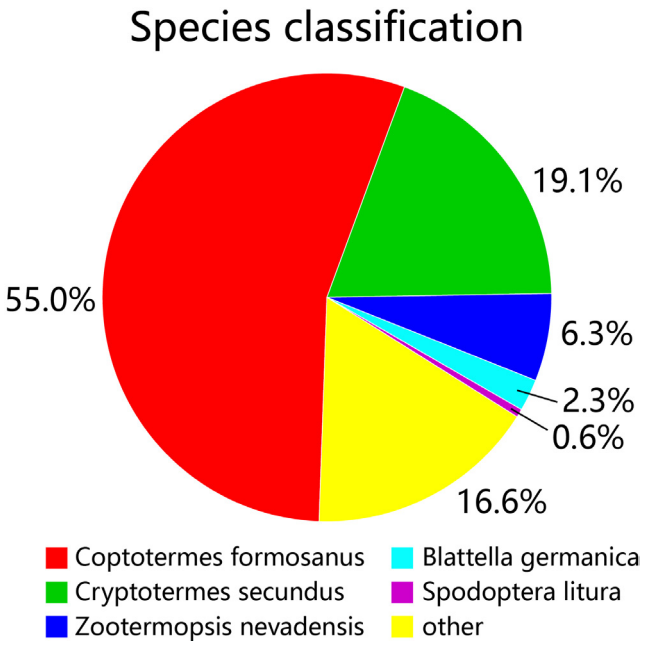

Fig 1. Nr classifications of all *C. formosanus.* Species distribution is shown as a percentage of the total homologous gene hits.

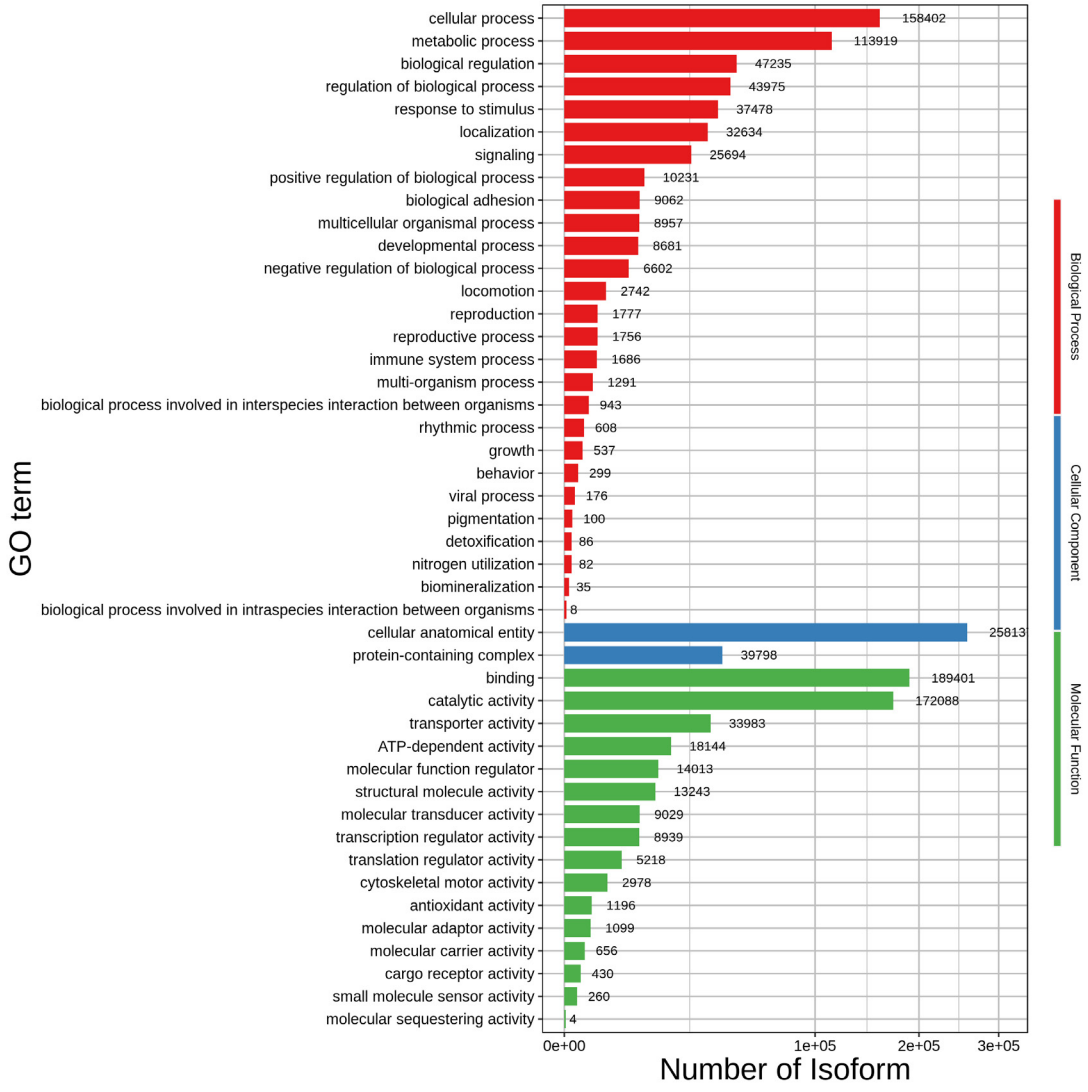

Fig 2. GO functional classifications of all *C. formosanus* unigenes. Red represents biological process; blue represents cellular component; and green represents molecular function. The x-axis represents GO categories; the y-axis (right) represents the number of transcripts.

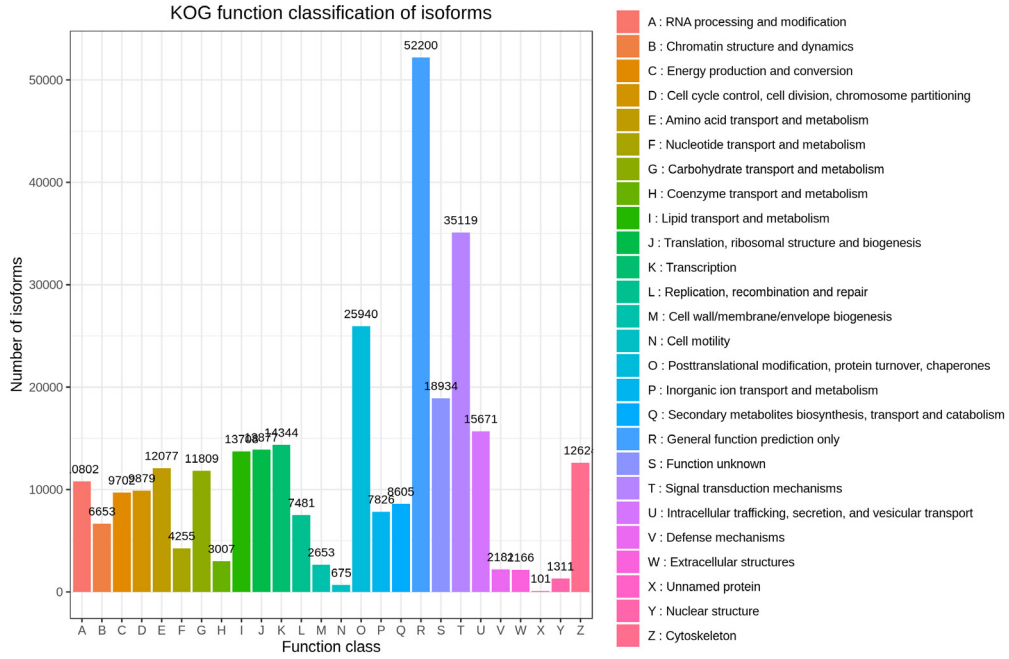

Fig 3. KOG annotations of putative proteins. The abscissa represents 26 KOG groups, and the ordinate shows the number of transcripts annotated to each group. The x-axis represents KOG categories; the y-axis represents the number of transcripts.

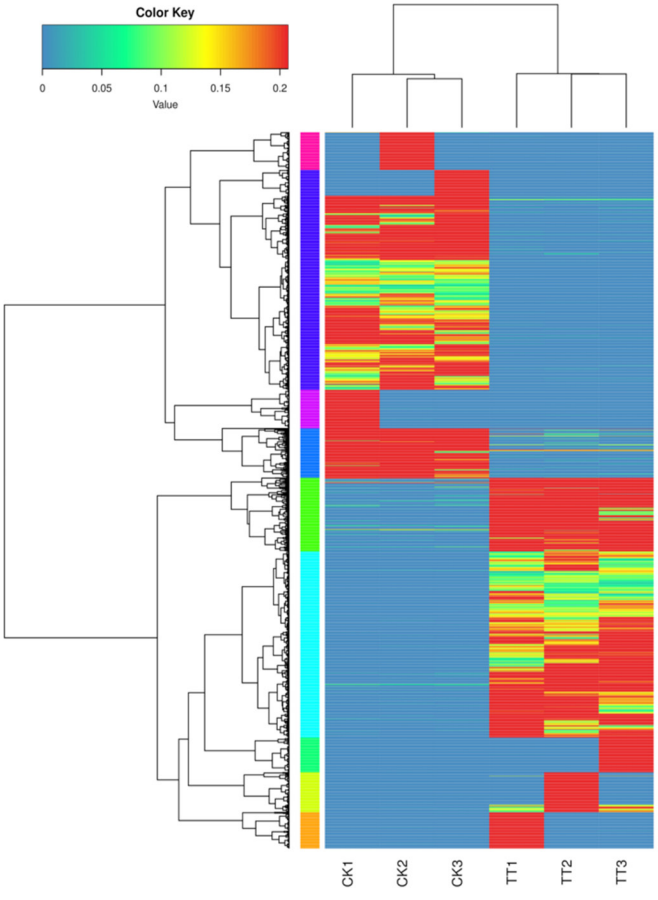

Fig 4. Overview of DEGs. A: Heatmaps illustrating differences in normalized log signal intensity for the identified *C. formosanus* genes. TT1, TT2 and TT3 are *A. lecanii* infection groups, and CK1, CK2 and CK3 are control groups. Red and blue indicate genes expressed at high and low levels, respectively. The colors from blue to red indicate gradually increasing expression.

DEGs in C. formosanus in response to A. lecanii infection

To elucidate the molecular mechanisms underlying *A. lecanii* infection, we employed the PacBio Sequel sequencing platform to identify differentially expressed genes (DEGs) in *C. formosanus* following infection. To maximize the accuracy of expression quantification, data from three biological replicates were merged for each condition, and the combined datasets were used to calculate fragments per kilobase of transcript per million mapped reads (FPKM) values. Differential expression analysis was then performed between the *A. lecanii*-infected group (TT) and the control group (CK) (Fig 4). In accordance with the screening criteria for DEGs, a total of 2782 DEGs were identified from the CK and TT groups (Fig 5), including 1440 upregulated genes and 1342 downregulated genes.

Analysis of immune-related DEGs

Among the DEGs, 56 immune-related genes were identified. These genes included 2 scavenger receptor genes, 5 apolipophorin genes, and one gene each encoding Cdc42, Integrin, and Toll. Additionally, 9 serine protease genes, 2 transferrin genes, 4 glutathione S-transferase (GST) genes, 28 cytochrome P450 genes, and 3 UDP-glucuronosyltransferase (UGT) genes were detected. Among these genes, 25 were downregulated, and 31 were upregulated (Table 3).

Gene Ontology (GO) analysis was conducted to classify the differentially expressed genes (DEGs) of *C. formosanus* according to their putative biological functions. A total of 2,782 DEGs were assigned to 36 functional categories across the three major GO domains: biological process (BP), cellular component (CC), and molecular function (MF) (Fig 6). Within the BP category, the most enriched subcategories were cellular

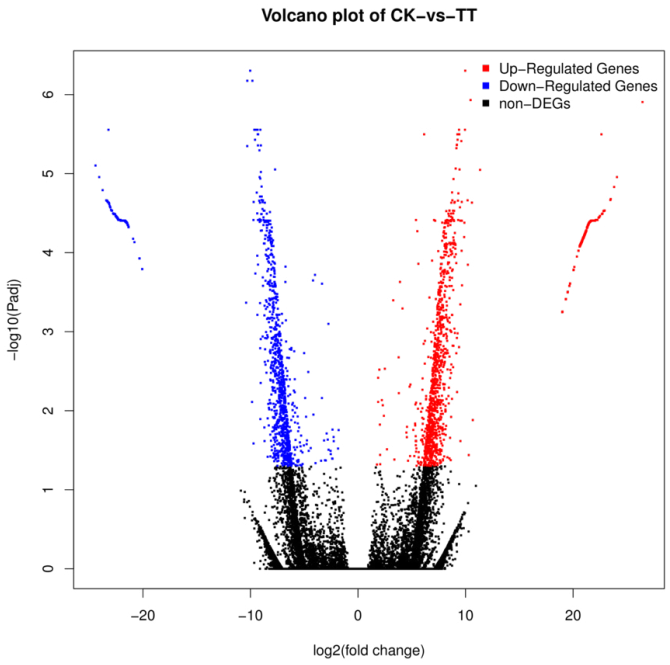

Fig 5. Comparison of gene expression levels between the CK and TT. Red and blue spots represent significantly up-regulated and down-regulated genes, respectively. Black spots indicate no significant differences in gene expression.

process (596 genes) and metabolic process (458 genes), followed by biological regulation (175 genes). In the CC category, the enriched subcategories were only cellular anatomical entities (997 genes) and protein-containing complexes (156 genes). For the MF category, the top three terms were binding (723 genes), catalytic activity (689 genes), and transporter activity (120 genes).

To investigate in greater detail which biological pathways of action participated in the response to *A. lecanii* infection, all the DEGs were mapped to the KEGG database. A total of 238 KEGG pathways were discovered (Fig 7), among which those with $p < 0.05$ were considered significantly enriched. Pathway enrichment analysis revealed that the DEGs were associated mainly with immune-related pathways. The top three enriched immune pathways included platelet activation (12 genes), neutrophil extracellular trap formation (11 genes), and chemokine signaling (11 genes). Additionally, genes involved in the MAPK signaling pathway were significantly enriched (Fig 8). These functional annotations provide valuable insights into the molecular responses of *C. formosanus* to *A. lecanii* infection and offer a foundation for further studies on termite immune defense and host-pathogen interactions.

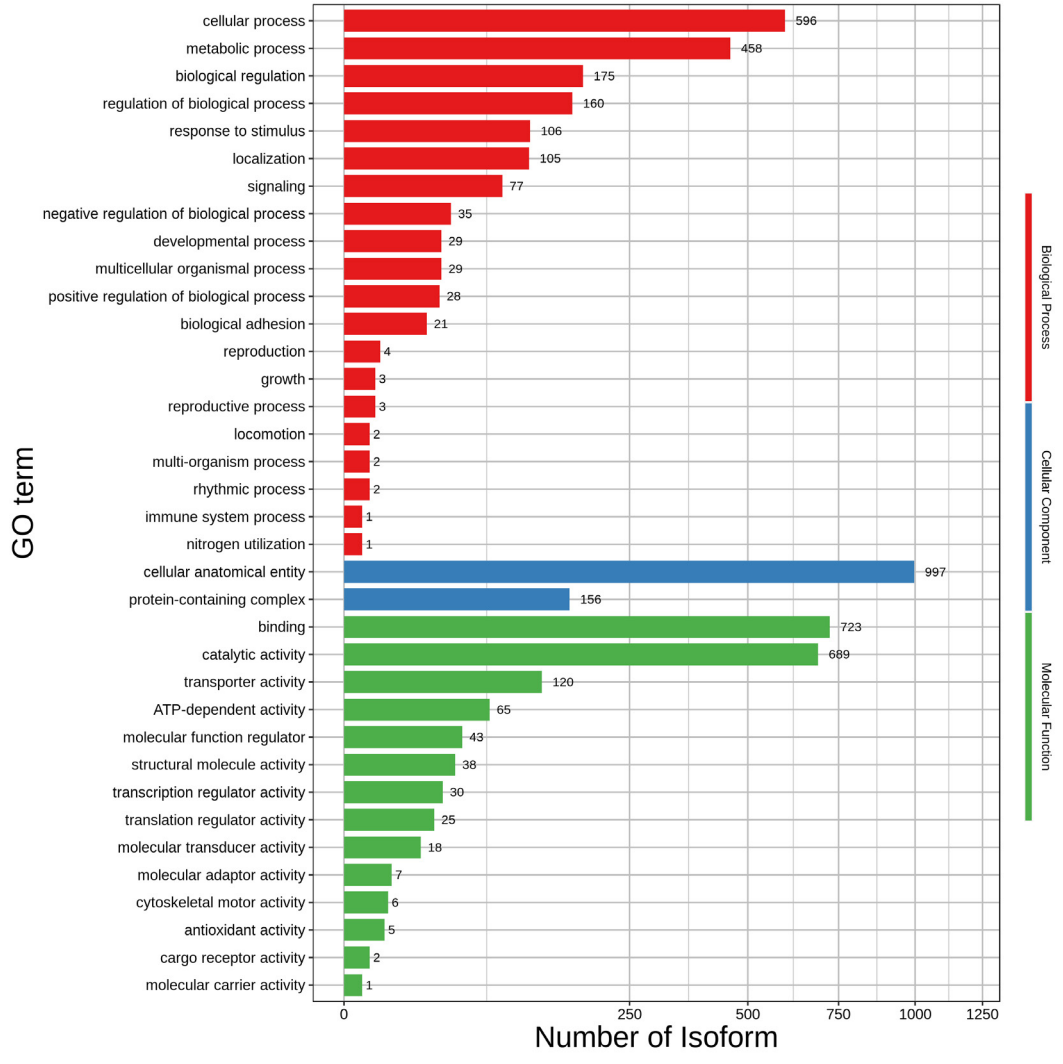

Fig 6. GO functional classification of DEGs in *C. formosanus*. Red represents biological process; blue represents cellular component; and green represents molecular function. The x-axis represents GO categories; the y-axis (right) represents the number of transcripts.

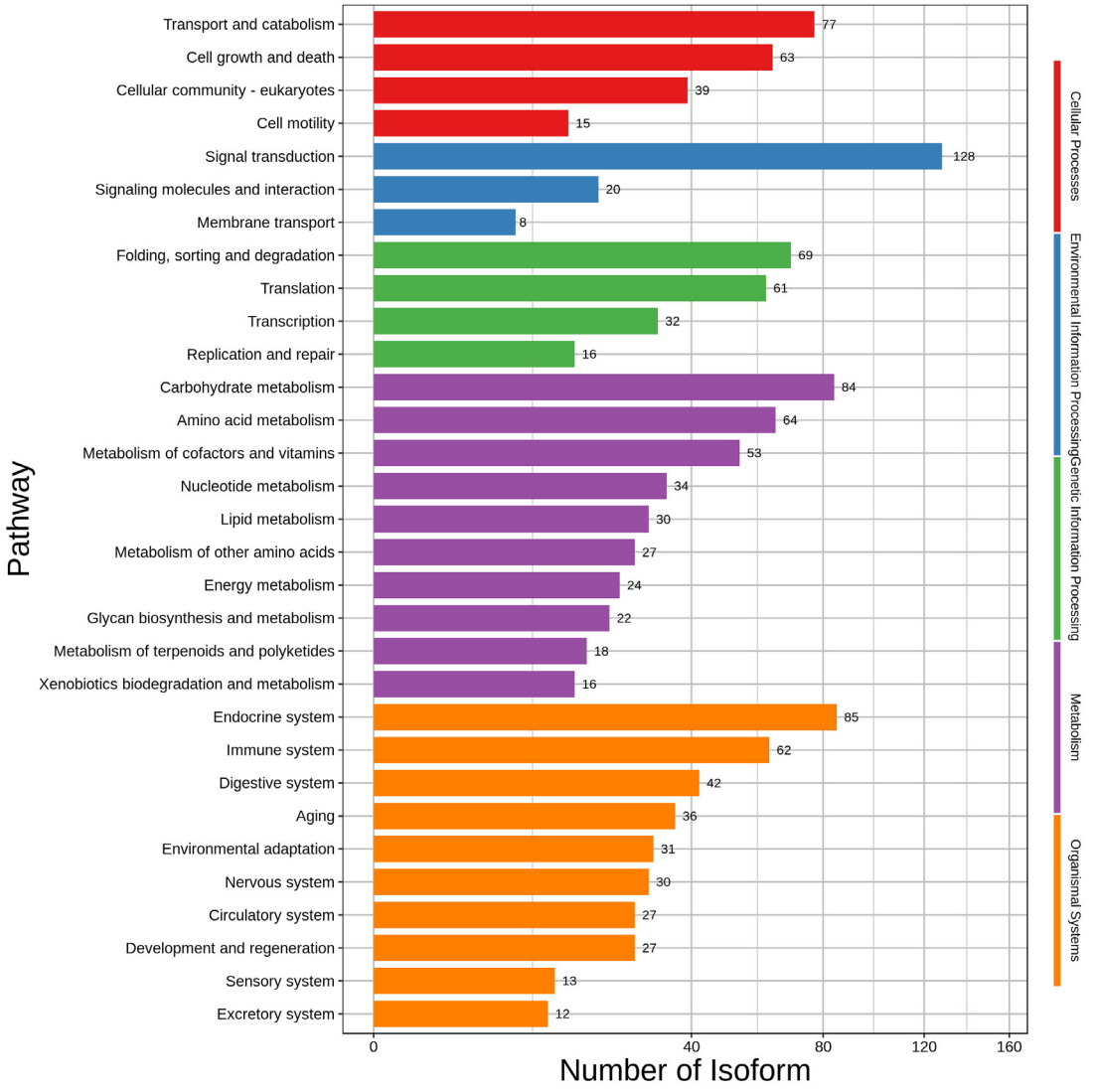

Fig 7. KEGG annotations of DEGs in *C. formosanus*. The x-axis represents KEGG pathway; the y-axis (right) represents the number of transcripts.

Discussion

This study is the first to use PacBio SMRT long-read sequencing technology to systematically analyze the full-length transcriptome dynamics of *C. formosanus* during *A. lecanii* infection. *A. lecanii* is a highly toxic entomopathogenic fungus isolated from termites. A large number of high-quality transcripts were obtained through analysis, of which more than 78% were functionally annotated in mainstream protein databases, clearly revealing the complex immune and metabolic remodeling processes of termites in response to fungal attacks. This work not only greatly contributes to the understanding of the genome annotation resources of *C. formosanus* but also provides a new perspective for understanding the fungal immune defense mechanisms of social insects at the molecular level.

In recent years, many studies have focused on termite biology and interactions with pathogens to improve pest management strategies (Lee et al., 2021). Previous studies have shown that termite immunity plays an important role in resistance to entomopathogenic fungi, such as *Metarhizium anisopliae* and *Beauveria bassiana*. For example, Chen et al. (2023) conducted a genome-wide analysis of *C. formosanus* after infection with *M. anisopliae* or nematodes and screened 104 immune genes related to *M. anisopliae* infection. Similarly, Zeng et al. (2024) reported that interfering with *Cfcat* expression played a crucial role in regulating innate immunity and could enhance the biocontrol effect of *M. anisopliae* on *C. formosanus*. Compared with these previous studies, our study revealed 2782 differentially expressed genes (DEGs), including 1440 upregulated and 1342 downregulated transcripts, indicating the activation of immune and metabolic responses in *C. formosanus* after infection with *A. lecanii*. Interestingly, a relative balance exists between upregulated and downregulated genes, and we speculate that this balance in the early stages of infection may be related to *A. lecanii* promoting infection by inhibiting the expression of termite-related genes and that the termite activates the immune

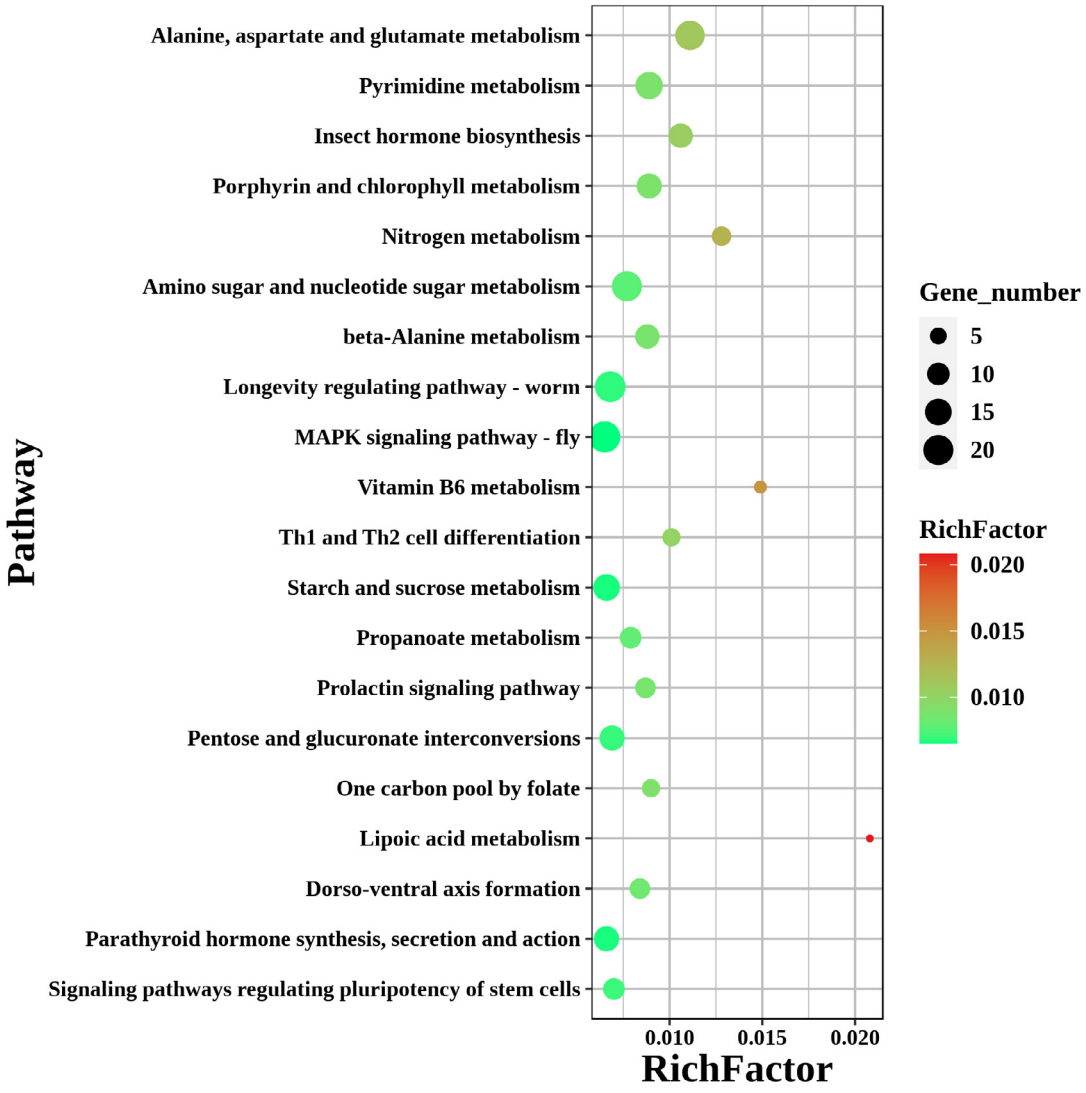

Fig 8. KEGG enrichment of DEGs in *C. formosanus*. The y-axis represents the name of the path, and the names are sorted from small to large according to Qvalue. The x-axis represents -log10 (Qvalue). The size of the point represents the number of differentially expressed genes in the path, and the color of the point corresponds to different rich factor ranges.

system to resist fungal invasion. However, importantly, the immune response is a dynamic process, and the use of a single time point represents a limitation of the present study. Future studies will incorporate multiple time points to better characterize the temporal dynamics of host-pathogen interactions.

Termites possess both individual immunity and social immunity. Social immunity is a distinctive defense strategy of eusocial insects and includes behaviors such as grooming, trophallaxis, and avoidance, which help reduce pathogen transmission within the colony. Previous studies have shown that exposure of termites to fungal infection significantly increases the frequency of social immune behaviors. For example, da Silva et al. (2025) reported that the frequency of social immune behaviors among infected termites is nearly four times greater than that among uninfected termites. In addition, Chen and Li (2025) reported that the downregulation of immune-related genes reduced social immune behaviors and increased mortality following *B. bassiana* infection. These findings suggest that social immunity plays an important role in colony-level defense.

Despite the importance of social immunity, individual immunity remains essential for protecting termites against microbial invasion (Cassidy et al., 2021). At the individual level, insect immunity consists of cellular and humoral responses. Cellular immunity includes phagocytosis, nodulation, and encapsulation, in which hemocytes directly interact with invading pathogens (Stanley et al., 2023). Humoral immunity is mediated mainly by conserved signaling pathways, including the Toll, immune deficiency (IMD), and JAK/STAT pathways (Elentherianos et al., 2021). In these pathways, pattern recognition receptors (PRRs) recognize pathogen-associated molecular patterns (PAMPs), activate downstream signaling cascades, and induce immune effectors such as antimicrobial peptides, melanization, and reactive oxygen species (Mahanta et al., 2023). The interaction between individual immunity and social immunity enables termites to maintain colony stability under pathogen pressure.

Consistent with this framework, our transcriptome analysis revealed significant changes in the expression of genes associated with innate immune signaling. PRR-mediated

recognition is a key initiating step that transmits signals to the nucleus to orchestrate immune responses (Pili-Floury et al., 2004). Multiple signaling pathways, such as the Toll, immune deficiency (IMD), Janus kinase/signal transducer and activator of transcription (JAK/STAT), and RNA interference (RNAi) pathways, transmit signals to the nucleus to coordinate immune responses (Lemaitre & Hoffmann, 2007; He et al., 2021). Among them, the Toll and IMD signaling pathways, both of which belong to the NF-κB signaling family, are central to humoral immunity because they regulate the synthesis of antimicrobial peptides (AMPs) (Govind, 2008; Kojour et al., 2020). The Toll signaling pathway is involved mainly in the immune response triggered by fungal, gram-positive bacterial, and viral infection, whereas the IMD signaling pathway is involved mainly in the immune response triggered by gram-negative bacteria. Toll and Toll-related proteins play critical roles in inducing AMP expression and thus mediate pathogen defense in insects. Toll receptors, as transmembrane proteins, profoundly influence insect development and innate immunity through NF-κB-dependent transcriptional regulation (Khan & Han, 2024). In our dataset, genes linked to the Toll pathway, including two scavenger genes, five apolipophorin genes, and one Toll receptor gene, exhibited notable transcriptional shifts. These changes suggest potential involvement in pathogen recognition and early immune responses to *A. lecanii*; however, transcriptomic signals alone do not play direct functional roles. We also observed a pronounced change in NF-κB gene expression, which may indicate the activation of nuclear transcriptional regulation by intracellular signaling. Overall, these results support the view that *C. formosanus* mounts an innate immune response upon fungal exposure but emphasize the need for functional validation to define gene-specific roles.

In addition, the Toll signaling pathway is closely related to not only the NF-κB pathway but also the MAPK signaling pathway. Guo et al. (2021) reported that the expression of various MAPK genes in *Plutella xylostella* (L.) significantly increased after infection by *Bacillus thuringiensis*, indicating that this pathway plays an important role in preventing infection by pathogenic bacteria. Consistent with these findings, three MAPK-related genes were identified, and two were significantly upregulated after *A. lecanii* infection. These findings suggest that MAPK signaling may contribute to antifungal defense in termites.

Recent research has indicated that immune-related genes are associated with social immunity in insects (Liu et al., 2023). In *O. formosanus*, suppression of the immune gene GNBP resulted in a marked reduction in the frequency of social immune behaviors following pathogen infection, leading to increased mortality (Feng et al., 2023). However, the present study is based solely on individual-level transcriptomic data and does not include behavioral assays. Therefore, although the differentially expressed immune genes identified here may be associated with immune processes that could influence social interactions, we cannot directly conclude that they regulate social immunity. Future studies integrating molecular analyses with quantitative behavioral approaches will be necessary to clarify the relationship between gene expression and social immunity. For example, computer vision–based multianimal tracking systems, such as DeepLabCut, could be used to precisely quantify changes in grooming frequency, trophallaxis, or social network structure following fungal infection. Such approaches would allow researchers to directly link transcriptional changes with colony-level behavioral responses and bridge the gap between molecular regulation and social immunity.

Apart from the classical immune signaling pathway, the melanization reaction also plays an important role in the immune response. This melanization reaction is dependent mainly on the prophenoloxidase (PPO) system, which is complex and provides broad-spectrum protection against fungi, parasites, and bacteria (Lu et al., 2014). In its inactive form, PPO is a zymogen, and upon infection by a pathogenic microorganism, PPO becomes proteolytically activated by serine proteases, thereby activating immune function. In *Aedes aegypti* (L.), the activation of the PPO system is evident after *B. bassiana* infection. This response is a manifestation of the activation of immune defense mechanisms (Ji et al., 2022). In contrast, an experiment on *Helicoverpa armigera* (Hübner) revealed that inhibition of the PPO pathway not only promoted fungal infectivity but also ultimately led to increased host lethality (Liu et al., 2021). Our transcriptomic data revealed that the expression of the nine serine protease genes in *C. formosanus* clearly decreased after *A. lecanii* infection. The observed data suggest that the fungus may secrete some products to prevent the activation of PPO, resulting in a reduction in the melanization ability of termites. Through such an effective strategy to circumvent the defense mechanism of termites, the possibility of hyphal expansion is increased, ultimately leading to the death of termites.

The humoral immunity of insects is an important barrier against the invasion of pathogenic microorganisms, and intricate cellular immunity provides additional reinforcement. For example, phagocytosis, encapsulation and nodulation are important components of cellular immunity. Infection with *M. anisopliae* has been reported to reduce the hemocyte count of *Spodoptera frugiperda* J. E. Smith and impair cellular immune defense (Wang et al., 2022). In our study, we revealed the upregulation of genes associated with cellular immunity, including ras homologous GTP-binding protein and integrin genes. We infer that these changes in gene expression indicate that upon infection with *A. lecanii*, the cellular immune response of *C. formosanus* is activated, further affecting signal transduction and pathogen phagocytosis.

In addition to classical immune signaling, the detoxification process is considered to be among the important components of the insect immune system (Kalil et al., 2017). Glutathione S-transferase (GST) transcripts have been reported to be upregulated in *Ixodes scapularis* Say cells upon *Anaplasma marginale* Theiler infection (de la Fuente et al., 2007). Similarly, cytochrome P450 expression increased

in *Brontispa longissima* (Gestro) following *M. anisopliae* infection (Wang et al., 2007). Consistent with these findings, our results revealed marked transcriptional changes in detoxification-related genes, including 4 GST genes (3 upregulated), 28 cytochrome P450 genes (17 upregulated), and 3 UDP-glucuronosyltransferase genes (2 upregulated), following *A. lecanii* infection. These findings indicate that *C. formosanus* may also increase its ability to detoxify fungal metabolites and do less harm to cells, so that a decrease in physiological damage can occur and physiological stability can be achieved under conditions of pathological stress.

Analysis of the transcriptome data indicated that *A. lecanii* infection successfully activated the immune response of *C. formosanus*. Apart from these findings, when *C. formosanus* was infected by this fungal pathogen, strong evidence of immune defensive ability was shown by *C. formosanus*. In response to infection, humoral immunity and cellular immune responses were activated or suppressed to some extent, thus reflecting the interrelationship and interaction of *C. formosanus* and *A. lecanii*. Therefore, with respect to detoxification-related enzyme-encoding genes, we observed that the detoxification metabolic defense is possibly also involved in resistance to infection by fungi. These observations highlight the role of termite immunity in response to invasion by any pathogenic organism. On the basis of these findings, more progressive molecular biology experimental methods should be employed to further study the immune interaction mechanism of *C. formosanus* with *A. lecanii*. The results of this investigation and the elucidation of these mechanisms can help improve the control of *C. formosanus* by *A. lecanii* and facilitate the identification of biological control factors using *A. lecanii* as a biological method for controlling the population of the pest.

Table 3. Immune-related genes among differentially expressed genes (DEGs).

Isoform_id	logFC		Gene name	Function
TT_mix_transcript_281579	21.12	up	Scavenger	Eliminate pathogens or apoptotic cells
TT_mix_transcript_203014	7.94	up	Scavenger	
TT_mix_transcript_52058	21.00	up	Apolipophorin	phagocytic recognition
TT_mix_transcript_5813	-7.84	down	Apolipophorin	
TT_mix_transcript_680853	-8.70	down	Apolipophorin	
TT_mix_transcript_558636	21.93	up	Apolipophorin	
TT_mix_transcript_362011	8.53	up	Apolipophorin	
TT_mix_transcript_213681	7.55	up	Cdc42	
TT_mix_transcript_89625	9.40	up	Integrin	
TT_mix_transcript_87417	-7.23	down	toll	
TT_mix_transcript_307465	-23.36	down	Serine protease	Prophenoloxidase（proPO）
TT_mix_transcript_1562645	-5.34	down	Serine protease	
TT_mix_transcript_205976	-6.58	down	Serine protease	
TT_mix_transcript_220476	-22.09	down	Serine protease	
TT_mix_transcript_369821	-6.35	down	Serine protease	
TT_mix_transcript_297711	-7.48	down	Serine protease	
TT_mix_transcript_1643945	-7.05	down	Serine protease	
TT_mix_transcript_1209152	6.56	up	Serine protease	
TT_mix_transcript_557636	-6.78	down	Serine protease	
TT_mix_transcript_571976	-21.65	down	Transferrin	Suppress pathogens
TT_mix_transcript_335875	20.36	up	Transferrin	
TT_mix_transcript_166253	7.84	up	Glutathione S-transferase	
TT_mix_transcript_1703891	21.56	up	Glutathione S-transferase	
TT_mix_transcript_403776	-8.50	down	Glutathione S-transferase	
TT_mix_transcript_33172	6.95	up	Glutathione S-transferase	
TT_mix_transcript_655411	-7.39	down	Cytochrome P450	
TT_mix_transcript_457385	-7.71	down	Cytochrome P450	
TT_mix_transcript_995780	7.83	up	Cytochrome P450	
TT_mix_transcript_68494	22.73	up	Cytochrome P450	
TT_mix_transcript_856704	-22.65	down	Cytochrome P450	

Table 3. Immune-related genes among differentially expressed genes (DEGs). (Continuation)

Isoform_id	logFC		Gene name	Function
TT_mix_transcript_137179	21.83	up	Cytochrome P450	
TT_mix_transcript_291966	-5.41	down	Cytochrome P450	
TT_mix_transcript_256718	-7.68	down	Cytochrome P450	
TT_mix_transcript_1703891	21.56	up	Cytochrome P450	
TT_mix_transcript_159471	8.03	up	Cytochrome P450	
TT_mix_transcript_8283	-22.11	down	Cytochrome P450	
TT_mix_transcript_874831	6.73	up	Cytochrome P450	
TT_mix_transcript_692188	6.67	up	Cytochrome P450	
TT_mix_transcript_1176074	20.80	up	Cytochrome P450	
TT_mix_transcript_1031189	7.03	up	Cytochrome P450	
TT_mix_transcript_128585	21.76	up	Cytochrome P450	
TT_mix_transcript_1102979	20.68	up	Cytochrome P450	
TT_mix_transcript_753699	-7.18	down	Cytochrome P450	Metabolism of toxins produced by microorganisms
TT_mix_transcript_1008516	21.20	up	Cytochrome P450	
TT_mix_transcript_778153	-6.60	down	Cytochrome P450	
TT_mix_transcript_319122	-6.25	down	Cytochrome P450	
TT_mix_transcript_62493	7.44	up	Cytochrome P450	
TT_mix_transcript_120223	-22.97	down	Cytochrome P450	
TT_mix_transcript_1080433	-8.08	down	Cytochrome P450	
TT_mix_transcript_1450091	8.01	up	Cytochrome P450	
TT_mix_transcript_1497587	20.84	up	Cytochrome P450	
TT_mix_transcript_900369	8.17	up	Cytochrome P450	
TT_mix_transcript_19348	8.75	up	Cytochrome P450	
TT_mix_transcript_137179	21.83	up	UDP-glucuronosyltransferase	
TT_mix_transcript_62493	7.44	up	UDP-glucuronosyltransferase	
TT_mix_transcript_706196	-7.19	down	UDP-glucuronosyltransferase	

Acknowledgements

This study was funded by the Ningbo "Kechuang Yongjiang 2035" Key Technology Research and Development Program (Grant No.2024Z274 & 2025Z096), the Scientific Research Project of Zhejiang Provincial Department of Education (Grant Y202352556), and the Scientific Research Project of NingBo City College of Vocational Technology (Grant ZZX23157).

Authors' Contribution

K. F: Conceptualization, methodology, funding acquisition, supervision, writing-original draft, writing-review & editing.
W. C.: Methodology.
Y. Z.: Investigation, project administration.
L. L.: Investigation.
F. Y.: Formal analysis.
Q. Y.: Formal analysis.
Y. H.: Investigation, funding acquisition.
Z. W.: funding acquisition.
W. L.: Writing-review & editing.

References

Cassidy, S.T., Chapa, J., Tran, T.A., Dolezal, N., Gerena, C., Johnson, G., Leyva, A., Stein, S., Wright, C.M. & Keiser, C.N. (2021). Disease defenses across levels of biological organization: individual and social immunity in acorn ants. Animal Behaviour, 179: 73-81. https://doi.org/10.1016/j.anbehav.2021.06.028

Chen, W. & Li, Z. (2025). miR-571 manipulating termite immune response to fungus and showing potential for green management of *Copotermes formosanus* (Blattodea: Isoptera). Pesticide Biochemistry and Physiology, 208: 106274. https://doi.org/10.1016/j.pestbp.2024.106274

Chen, W.W., Zeng, W.H., Shen, D.N., Feng, S.Y. & Li, Z.Q. (2023). Genome-wide identification of *Coptotermes formosanus* immune genes and their potential roles in termite control. Gene, 877: 147569. https://doi.org/10.1016/j.gene.2023.147569

da Silva, L.H.B., Goes, A.C., Rodrigues, A., Fourcassié, V., McMahon, D. & Haifig, I. (2025). Social immune response

reflects infection progression in a soldierless termite. Behavioral Ecology and Sociobiology, 79: 11. https://doi.org/10.1007/s00265-024-03556-2

de la Fuente, J., Blouin, E.F., Manzano-Roman, R., Naranjo, V., Almazan, C., Pérez de la Lastra, J.M., Zivkovic, Z., Jongejan, F. & Kocan, K.M. (2007). Functional genomic studies of tick cells in response to infection with the cattle pathogen, *Anaplasma marginale*. Genomics, 90: 712-722. https://doi.org/10.1016/j.ygeno.2007.08.009

Eleftherianos, I., Heryanto, C., Bassal, T., Zhang, W., Tettamanti, G. & Mohamed, A. (2021). Haemocyte-mediated immunity in insects: Cells, processes and associated components in the fight against pathogens and parasites. Immunology, 164: 401-432. https://doi.org/10.1111/imm.13390

Feng, K., Jiang, D., Luo, J. & Tang, F. (2023). OfGNBP silencing enhances the toxicity of Serratia marcescens Bizio (SM1) to *Odontotermes formosanus* (Shiraki). Pesticide Biochemistry and Physiology, 189: 105306. https://doi.org/10.1016/j.pestbp.2022.105306

Feng, K., Lu, X., Luo, J. & Tang, F. (2020). SMRT sequencing of the full-length transcriptome of *Odontotermes formosanus* (Shiraki) under Serratia marcescens treatment. Scientific Reports, 10: 15909. https://doi.org/10.1038/s41598-020-73075-3

Gao, S., Ren, Y., Sun, Y., Wu, Z.F., Ruan, J.S., He, B.J., Zhang, T., Yu, X., Tian, X.X. & Bu, W.J. (2016). PacBio full-length transcriptome profiling of insect mitochondrial gene expression. RNA Biology, 13: 820-825. https://doi.org/10.1080/15476286.2016.1197481

Govind, S. (2008). Innate immunity in Drosophila: Pathogens and pathways. Insect Science, 15: 29-43. https://doi.org/10.1111/j.1744-7917.2008.00185.x

Guo, Z., Kang, S., Wu, Q., Wang, S., Crickmore, N., Zhou, X., Bravo, A., Soberón, M. & Zhang, Y. (2021). The regulation landscape of MAPK signaling cascade for thwarting *Bacillus thuringiensis* infection in an insect host. PLoS Pathogens, 17: e1009917. https://doi.org/10.1371/journal.ppat.1009917

He, Y.J., Lu, G., Qi, Y.H., Zhang, Y., Zhang, X.D., Huang, H.J., Zhuo, J.C., Sun, Z.T., Yan, F., Chen, J.P., Zhang, C.X. & Li, J.M. (2021). Activation of Toll Immune Pathway in an Insect Vector Induced by a Plant Virus. Frontiers in Immunology, 11: 613957. https://doi.org/10.3389/fimmu.2020.613957

Hu, Y.X., Wang, Y., Deng, J.P. & Jiang, H.B. (2016). The structure of a prophenoloxidase (PPO) from Anopheles gambiae provides new insights into the mechanism of PPO activation. BMC Biology, 14: 2. https://doi.org/10.1186/s12915-015-0225-2

Ji, Y., Lu, T., Zou, Z. & Wang, Y. (2022). Aedes aegypti CLIPB9 activates prophenoloxidase-3 in the presence of CLIPA14 after fungal infection. Frontiers in Immunology, 13: 927322. https://doi.org/10.3389/fimmu.2022.927322

Jia, D., Wang, Y., Liu, Y., Hu, J., Guo, Y.Q., Gao, L.L. & Ma, R.Y. (2018). SMRT sequencing of full-length transcriptome of flea beetle *Agasicles hygrophila* (Selman and Vogt). Scientific Reports, 8: 2197. https://doi.org/10.1038/s41598-018-20181-y

Kalil, S.P., Rosa, R.D., Capelli-Peixoto, J., Pohl, P.C., Oliveira, P.L., Fogaça, A.C. & Daffre, S. (2017). Immune-related redox metabolism of embryonic cells of the tick *Rhipicephalus microplus* (BME26) in response to infection with Anaplasma marginale. Parasites & Vectors, 10: 613. https://doi.org/10.1186/s13071-017-2575-9

Kalleshwaraswamy, C.M., Shanbhag, R.R. & Sundararaj, R. (2022). Wood degradation by termites: Ecology, economics, and protection. Science of Wood Degradation and its Protection (pp.147-170). Singapore: Springer Singapore. https://doi.org/10.1007/978-981-16-8797-6_5

Kepler, R.M., Jennifer, L.A.J., Hywel-Jones, N.L., Quandt, C.A., Sung, G.H., Rehner, S.A., Aime, M.C., Henkel, T.W., Sanjuan, T., Zare, R., Chen, M.J., Li, Z.Z., Rossman, A.Y., Spatafora, J.W. & Shrestha, B. (2017). A phylogenetically-based nomenclature for Cordycipitaceae (Hypocreales). IMA Fungus, 8: 335-353. https://doi.org/10.5598/imafungus.2017.08.02.08

Khan, S.A. & Han, Y.S. (2024). Current status of innate immune responses in Malpighian tubules of insects: A review focusing on the Toll signaling pathway. Entomological Research, 54: e12716. https://doi.org/10.1111/1748-5967.12716

Kojour, M.A.M., Han, Y.S., Hun, Y.J. & Jo, Y.H. (2020). An overview of insect innate immunity. Entomological Research, 50: 282-291. https://doi.org/10.1111/1748-5967.12437

Lee, S.B., Tong, R.L., Kim, S.H., Im, I.G. & Su, N.Y. (2021). Potential pest status of the Formosan subterranean termite, *Coptotermes formosanus* Shiraki (Blattodea: Isoptera: Rhinotermitidae), in response to climate change in the Korean Peninsula. Florida Entomologist, 103: 431-437. https://doi.org/10.1653/024.103.00403

Lemaitre, B. & Hoffmann, J. (2007). The host defense of *Drosophila melanogaster*. Annual Review of Immunology, 25: 697-743. https://doi.org/10.1146/annurev.immunol.25.022106.141615

Liu, L., Yan, F.M., Zhao, C.C., Su, L.J., Huang, Q.Y. & Tang, Q.B. (2023). microRNAs shape social immunity: a potential target for biological control of the termite *Reticulitermes chinensis*. Journal of Pest Science, 96: 265-279. https://doi.org/10.1007/s10340-022-01495-3

Liu, Z.C., Zhou, L., Wang, J.L. & Liu, X.S. (2021). Expression of a phenoloxidase cascade inhibitor enhances the virulence of the fungus *Beauveria bassiana* against the insect *Helicoverpa armigera*. Developmental & Comparative Immunology, 117: 103986. https://doi.org/10.1016/j.dci.2020.103986

Lu, A., Zhang, Q., Zhang, J., Yang, B., Wu, K., Xie, W., Luan, Y.X. & Ling, E. (2014). Insect prophenoloxidase: the view

beyond immunity. Frontiers in physiology, 5: 252. https://doi.org/10.3389/fphys.2014.00252

Mahanta, D.K., Bhoi, T.K., Komal, J., Samal, I., Nikhil, R.M., Paschapur, R.N., Singh, G., Kumar, P.V.D., Desai, D.R., Ahmad, M.A., Singh, P.P., Majhi, P.K., Mukherjee, U., Singh, P., Saini, V., Shahanaz, Srinivasa, N. & Yele, Y. (2023). Insect-pathogen crosstalk and the cellular-molecular mechanisms of insect immunity: uncovering the underlying signaling pathways and immune regulatory function of non-coding RNAs. Frontiers in Immunology, 14: 1169152. https://doi.org/10.3389/fimmu.2023.1169152

Merkling, S.H. & van Rij, R.P. (2013). Beyond RNAi: antiviral defense strategies in *Drosophila* and mosquito. Journal of Insect Physiology, 59: 159-170. https://doi.org/10.1016/j.jinsphys.2012.07.004

Pili-Floury, S., Leulier, F., Takahashi, K., Saigo, K., Samain, E., Ueda, R. & Lemaitre, B. (2004). In Vivo RNA Interference Analysis Reveals an Unexpected Role for GNBP1 in the Defense against Gram-positive Bacterial Infection in *Drosophila* Adults. Journal of Biological Chemistry, 279: 12848-12853. https://doi.org/10.1074/jbc.m313324200

Sharma, A., Sharma, S. & Yadav, P.K. (2023). Entomopathogenic fungi and their relevance in sustainable agriculture: A review. Cogent Food & Agriculture, 9: 2180857. https://doi.org/10.1080/23311932.2023.2180857

Sharma, I., Sharma, A. & Sharma, S. (2025). Role of Termites in Waste Management: Current Progress and Future Potential. Waste Management: From Trash to Treasure, 125p.

Stanley, D., Haas, E. & Kim, Y. (2023). Beyond cellular immunity: on the biological significance of insect hemocytes. Cells, 12: 599. https://doi.org/10.3390/cells12040599

Wang, J.H., Huang, J.S. & Fang, X.D. (2007). Identification and induction by *Metarhizium anisopliae* infection of family4 cytochrome P450 in *Brontispa longissimi*. Acta Entomologica Sinica, 50: 14-19.

Wang, J.L., Yang, K.H., Wang, S.S., Li, X.L., Liu, J., Yu, Y.X. & Liu, X.S. (2022). Infection of the entomopathogenic fungus Metarhizium rileyi suppresses cellular immunity and activates humoral antibacterial immunity of the host Spodoptera frugiperda. Pest Management Science, 78: 2828-2837. https://doi.org/10.1002/ps.6907

Xu, S., Duan, Y., Ma, L., Song, F., Tian, L., Cai, W.Z. & Li, H. (2023). Full-length transcriptome profiling of *Coridius chinensis* mitochondrial genome reveals the transcription of genes with ancestral arrangement in insects. Genes, 14: 225. https://doi.org/10.3390/genes14010225

Xue, Y., Li, H. & Kang, X. (2024). Molecular unraveling of polysaccharide digestion in wood-feeding termites: A solid-state NMR perspective. Carbohydrate Polymers, 331: 121843. https://doi.org/10.1016/j.carbpol.2024.121843

Zeng, W., Shen, D., Wu, W., Zhang, S.J., Li, Z.Q. & Zhang, D.D. (2024). Involvement of a catalase gene in lignin catalysis and immune defense against pathogenic fungus in *Coptotermes formosanus*: a potential new target for termite control. Pest Management Science, 80: 3258-3268. https://doi.org/10.1002/ps.8029